

Probing gas and dust in the tidal tail of NGC 5221 with the type Ia supernova iPTF16abc[★]

R. Ferretti¹, R. Amanullah¹, A. Goobar¹, T. Petrushevska¹, S. Borthakur, Y. Cao, O. Fox, E. Freeland, C. Fremling, G. Hosseinzadeh, and more

Department of Physics, The Oskar Klein Centre, Stockholm University, Albanova, SE 106 92 Stockholm, Sweden
e-mail: raphael.ferretti@fysik.su.se

Received ... ; accepted ...

ABSTRACT

Context. Type Ia supernovae (SNe Ia) can be used to address numerous questions in astrophysics and cosmology. Due to their well known spectral and photometric properties, SNe Ia are well suited to study gas and dust along the lines-of-sight to the explosions. For example, narrow Na I D and Ca II H&K absorption lines can easily be studied, because of the well defined spectral continuum of SNe Ia around these features.

Aims. We study the gas and dust along the line-of-sight to iPTF16abc, which occurred in an unusual location, in a tidal arm, 80 kpc from the galaxy NGC 5221.

Methods. Using a time-series of high-resolution spectra, we examine narrow Na I D and Ca II H&K absorption features for variations in time, which would be indicative for circumstellar (CS) matter. Furthermore, we take advantage of the well known photometric properties of SNe Ia to determine reddening due to dust along the line-of-sight.

Results. From the lack of variations in Na I D and Ca II H&K, we determine that none of the detected absorption features originate from the CS medium of iPTF16abc. While the Na I D and Ca II H&K absorption is found to be optically thick, a negligible amount of reddening points to a small column of interstellar dust. We further detect a diffuse interstellar band (DIB) at $\lambda 6284$, which may be the first such detection in a tidal tail of a galaxy.

Conclusions. We find that the gas along the line-of-sight to iPTF16abc is typical of what might be found in the interstellar medium (ISM) within a galaxy. It suggests that we are observing gas that has been tidally stripped during an interaction of NGC 5221 with one of its neighbouring galaxies in the past $\sim 10^9$ years. In future, the gas clouds could become the locations of star formation. On a longer time scale, the clouds might diffuse, enriching the circum-galactic medium (CGM) with metals. The gas profile along the line-of-sight should be useful for future studies of the dynamics of the galaxy group containing NGC 5221.

Key words. supernovae: individual: iPTF16abc – circumstellar matter – Galaxies: individual: NGC 5221 – Galaxies: ISM

1. Introduction

Type Ia supernovae (SNe Ia) have such uniform properties that they are frequently described as "standard candles", which, among other applications, enables detailed measurements in cosmology (see for instance Goobar & Leibundgut 2011). The well-known brightness and spectral energy distribution (SED) of SNe Ia can also be used to study gas and dust along the lines-of-sight.

Due to the well defined continuum of SNe Ia, typical absorption features of the interstellar medium (ISM) of their host galaxies, such as Na I D and Ca II H&K, can frequently be identified. Furthermore, diffuse interstellar bands (DIBs), which are largely of unknown chemical origin (Snow 2001; Snow & McCall 2006), are sometimes detected in the spectra (e.g. Sollerman et al. 2005). We take advantage of the standard candle properties of SNe Ia to study dust. Comparing the lightcurves of a given SN Ia with an SED template, extinction and reddening can be determined to study the dust properties along the line-of-sight.

For example, the nearest SN Ia in modern times, SN 2014J, (Goobar et al. 2014), has been used to study details of the ISM

composition of M82 (Welty et al. 2014; Ritchey et al. 2015). Furthermore, an unusual extinction curve was identified which possibly points to very small dust grains in the ISM or dust in the circumstellar (CS) medium of the supernova (Amanullah et al. 2014; Foley et al. 2014).

SNe Ia can be used to study a large variety of lines-of-sight. Due to the large delay times of $\approx 10^8$ – 10^9 years between the formation of a SN Ia progenitor system and the explosion (Maoz et al. 2012), they are known to occur almost anywhere in their host galaxies. An extreme example is PTF10ops, which was located at a projected distance of 148 kpc from the nearest possible host galaxy (Maguire et al. 2011).

It is thus possible for SNe Ia to occur in regions with low stellar density, such as tidally stripped spiral arms of a galaxies. Tidal arms are thought to be the result of close interactions of neighbouring galaxies (as shown in the simulations by Toomre & Toomre 1972). SNe Ia occurring in such locations can be used to study the interstellar gas and dust properties of regions that have been affected by gravitational interactions. The ISM in tidal arms can be the location of future star formation (Schombert et al. 1990) and enrich the circumgalactic medium (CGM) with metals.

To date no SN Ia located in a tidal arm has been studied in detail, although at least one case is known (SN 2013de, Drake

[★] Based on observations collected at the European Organisation for Astronomical Research in the Southern Hemisphere under ESO DDT programme 297.D-5005(A), P.I. Ferretti.

et al. 2013a,b). Here we investigate iPTF16abc, a SN Ia which occurred in the tidal arm of its host galaxy NGC 5221. Due to the large displacement of iPTF16abc from its host, the supernova was a good candidate to search for the presence of CS gas via photoionisation using the method described in Ferretti et al. (2016). Furthermore, the obtained high-resolution spectra and photometry could be used to study the spiral arm it is located in.

In the following, we present the discovery and observations of iPTF16abc (Section 2). We then describe the narrow absorption features detected in high-resolution spectra, as well as the photometric reddening of iPTF16abc (Section 3). We further show that the deep absorption features cannot be due to CS gas surrounding the supernova, but are part of the tidally stripped ISM of NGC 5221 (Section 4). Finally, we compare the line-of-sight with NGC 5221 and discuss the features in the context of the galaxy group NGC 5221 is located in (Sections 5 and 6).

2. Discovery and Observations of iPTF16abc

The intermediate Palomar Transient Factory (iPTF) first reported the discovery of iPTF16abc (Miller et al. 2016), located $170''$ from the galaxy NGC 5221 at R.A., Dec = 13:34:45.492 +13:51:14.30 (J2000), a line-of-sight that has low Milky Way reddening with $E(B - V)_{MW} = 0.028$ (Schlafly & Finkbeiner 2011). A colour composite image of NGC 5221 and the location of iPTF16abc is shown in Figure 1. The supernova was discovered on 4.4 April 2016, while the first detection was on 3.4 April and the last non-detection occurred on 2.4 April (UT dates are used throughout the paper).

A classification spectrum of iPTF16abc was obtained with the DeVeny spectrograph on the Discovery Channel Telescope (DCT) (Cenko et al. 2016) on 5.3 April, which determined it to be a SN Ia, possibly belonging to the subclasses resembling SNe 1991T or 1999aa. A spectrum obtained with Gemini N+GMOS on 5.4 April revealed the presence of deep Na I D and Ca II H&K absorption features. In response, extensive photometric and spectroscopic follow-up were triggered (Cao 2017, in prep.).

As part of the follow-up of iPTF16abc, we received Directors Discretionary Time at the European Organisation for Astronomical Research in the Southern Hemisphere (ESO DDT programme 297.D-5005(A), P.I. Ferretti). The spectra taken with Xshooter ($R \approx 7500$ Vernet et al. 2011) and the Ultraviolet and Visual Echelle Spectrograph (UVES; $R \approx 50000$ Dekker et al. 2000) both on Kueyen (UT2) 8.2 m unit at the Very Large Telescope (VLT) are summarised in Table 1. The Xshooter and UVES spectra were reduced using the REFLEX (ESOREX) reduction pipeline provided by ESO (Modigliani et al. 2010). Where necessary, telluric features were corrected for using Molecfit (Smette et al. 2015; Kausch et al. 2015).

We analyse the photometry of iPTF16abc, which will be presented in Cao (2017, in prep.). From the Palomar Observatory 48-inch telescope (P48) we use g - and R -band photometry which was obtained as part of the regular iPTF survey. Further we use gr - and i -band photometry of the Palomar Observatory 60-inch telescope (P60) and $BVgr$ - and i -band from the Las Cumbres Observatory Global Telescope (LCOGT). Ultraviolet (UV) photometry from the Ultraviolet/Optical Telescope (UVOT; Roming et al. 2005) on the *Swift* spacecraft (Gehrels et al. 2004) $uvm2$ -filter and $riZYZ$ - and H -band with the Reionisation and Transient Infrared/Optical Project (Fox et al. 2012) were obtained and was used for this analysis.

3. Absorption features and reddening

Deep well-defined narrow absorption lines corresponding Na I D and Ca II H&K at the rest frame of NGC 5221 ($z = 0.0234$, Courtois & Tully 2015) are evident in all Xshooter and UVES spectra obtained. We detect two distinct groups of absorbers at different radial velocities in the UVES spectra. The absorption line profiles can be seen in Figure 2, where the two deep feature groups are centred at a radial velocity $v_r \approx -77$ and -51 km s $^{-1}$, with respect to the host galaxy rest frame.

Both groups of absorption line features are visibly asymmetric, indicating that the absorption features are composed of several blended components. Unfortunately, the lines are too saturated and blended to determine any further substructure with confidence. Consequently, only lower limits of the column densities of the absorbers could be determined. Both Na I D and Ca II H&K can be considered to be optically thick, since their line ratios (D2 / D1 and K / H) are much lower than 2, while the corresponding transitions have oscillator strength ratios of 2-to-1 (Kramida et al. 2014). The equivalent widths (EWs) and column density lower limits of the two absorption feature groups are presented in Table 2.

Furthermore we detect a common DIB at $\lambda 6284$, of which we measure an $EW_{\lambda 6284} = 150 \pm 30$ mÅ, by assuming a Gaussian profile and polynomial continuum. Interestingly, the DIB at $\lambda 6284$ is also detected in other SNe (e.g. 2001el, 2013gh and 2014J Sollerman et al. 2005; Ferretti et al. 2016; Welty et al. 2014, respectively), but is not necessarily detected in any galaxy, as the example of Ritchey & Wallerstein (2015) in M51 shows. Other known DIBs, such as $\lambda \lambda 5780$ and 5797 , which are believed to correlate well with reddening (Phillips et al. 2013; Baron et al. 2015), are not detectable above the noise level. Assuming a full-width-half-maxima from SN 2001el for DIBs $\lambda \lambda 5780$ and 5797 of 2.0 and 0.7 Å, the corresponding EWs must be < 150 and < 50 mÅ, respectively given the signal-to-noise ratio.

We further detect K I at $\lambda \lambda 7667$ and 7701 in the Xshooter spectra. From the spectrum obtained on 4 April, we measure EWs = 112 ± 9 and 71 ± 6 mÅ, respectively. While the K I is also visible in the spectrum from 12 May, several noisy features that do not correspond to telluric lines make precise EW measurements difficult.

From the UV, optical and IR photometry of iPTF16abc we can estimate the reddening of the SN by fitting the SED of SN 2011fe (as in Amanullah et al. 2014, 2015) to the data. Aside from the unusually fast rise of iPTF16abc, the above SED fits the lightcurve and colours well. For this reason, we avoid including the early photometry and the light-curves using the photometry between phases $p = -10 - +40$ days.

The measured reddening is estimated to $E(B - V) = 0.07$ (0.05) for $R_V = 1.4$ (3.1), i.e. the full range of $R_V = 1.4-3.1$ values measured for SNe Ia (e.g. Amanullah et al. 2015). The fit further determined the light-curve parameters $t_{B_{\max}} = 57498.76$ and $s = 1.074$, which define the B-band maximum brightness in MJD and the lightcurve stretch with respect to SN 2011fe (see e.g. Goldhaber et al. 2001, for a discussion on lightcurve stretch), respectively. All statistical uncertainties are subdominant, and the errors are dominated by the assumed value of R_V . The fitted values of $E(B - V)$ correspond to an extinction of $A_V = 0.1$ (0.2).

The extinction can also be estimated by taking advantage of the standard candle property of SNe Ia and comparing the measured peak brightness with the expected for the given redshift, $z = 0.0234$, of NGC 5221. Using SNe Ia lightcurve fitter SALT2 (Guy et al. 2007), we find that $A_V = -0.03 \pm 0.04$ which is

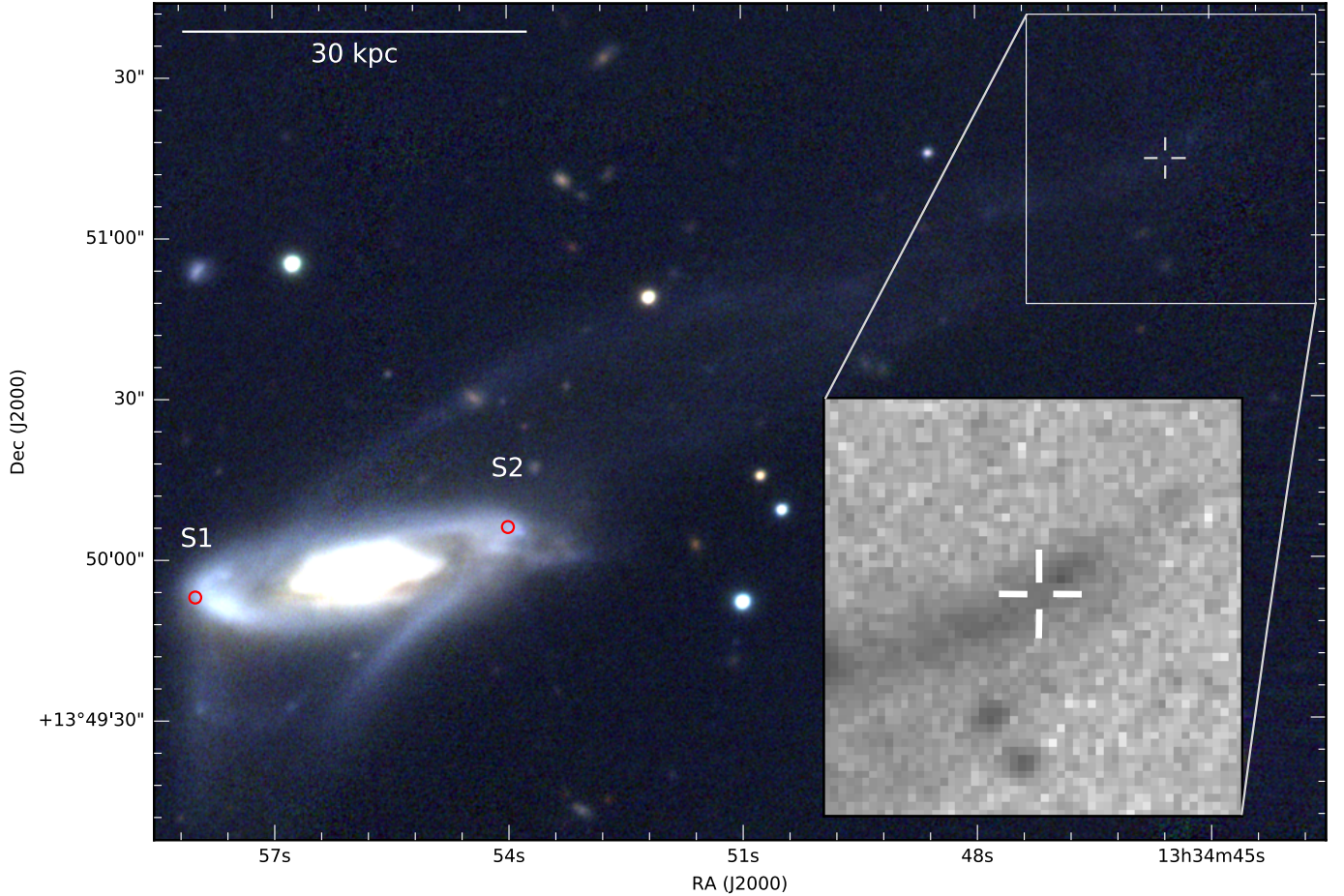


Fig. 1. The location of iPTF16abc, marked in the inset, with respect to its host galaxy NGC 5221. The tidal tail is visible spanning the space between the galaxy and the supernova location. Coordinates at which SDSS spectra of NGC 5221 are available are marked and labeled S1 and S2. The main image is a colour composite of the publicly available PanSTARRS data (Flewelling et al. 2016). The inset is a deep stack of iPTF P48 R-band images.

Instrument	MJD	UT Date	Exp. time (s)	Phase (days)	Set-up
Xshooter	57,492.7	Apr. 14.7	1755	-6.1	UVB 1.0"/VIS 0.9"/NIR 0.9"
UVES	57,495.2	Apr. 17.2	2×1700	-3.6	0.8" DIC1 390+580
UVES	57,503.1	Apr. 25.1	3450	4.3	0.8" DIC1 390+580
Xshooter	57,520.0	May 12.0	1829	21.2	UVB 1.0"/VIS 0.9"/NIR 0.9"

Table 1. Mid- and high-resolution spectra obtained with stretch-corrected phases in the rest frame with respect to B-band maximum.

well within the expected intrinsic peak brightness dispersion of 0.1 mag.

In the past, grey dust ejected from galaxies has been proposed (Aguirre 1999a,b; Goobar et al. 2002) as an alternative explanation to the observations interpreted as a cosmological constant driven acceleration of the universe (Perlmutter et al. 1999; Riess et al. 1998). Although quasar observations have shown that grey dust is not responsible for the dim appearance of cosmological SNe Ia samples (Mörtsell & Goobar 2003; Ménard et al. 2010), a small grey dust component could still lead to biased measurements of cosmological samples. Matter streaming from a galaxy is a suggested location where grey dust could be forming. In such a scenario the line-of-sight to iPTF16abc should probe and overdensity of grey dust, and the standard candle properties of this SN Ia can be used to constrain it. Since the peak

brightness of iPTF16abc is within the intrinsic scatter of SNe Ia however, the grey dust column along the line-of-sight must be negligible.

4. Absence of circumstellar absorption

Although the majority of the absorption lines detected in SNe Ia spectra are believed to be due to gas in the interstellar medium of their host galaxies, there exist observations that indicate the presence of CS gas. For example, cases of slight variations in absorption line profiles (Patat et al. 2007; Simon et al. 2009; Graham et al. 2015; Ferretti et al. 2016) hint at photoionisation or recombination and predominantly blue-shifted Na I D profiles (Sternberg et al. 2011; Maguire et al. 2013) suggest outflowing gas.

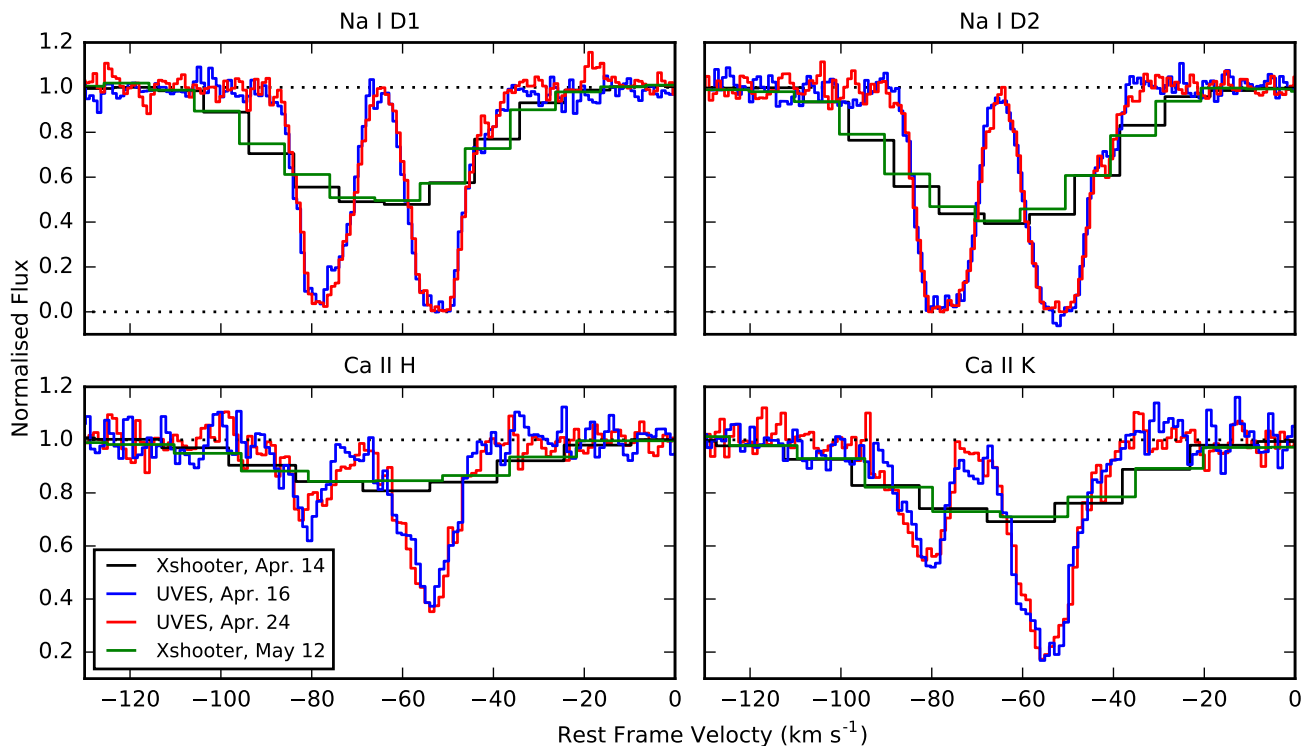


Fig. 2. The Na I D doublet and Ca II H&K of iPTF16abc by UVES and Xshooter. In the UVES spectra, two distinct groups of absorption features with similar velocities are visible, while they are unresolved by Xshooter. The substructure of these groups is difficult to further discern due to the optical thickness of the absorbers.

v	Na I D1	Na I D2	ratio	$N(\text{Na I})^\dagger$	Ca II H	Ca II K	ratio	$N(\text{Ca II})^\ddagger$
(km/s)	(mÅ)	(mÅ)	(D2/D1)	($\times 10^{12} \text{ cm}^{-2}$)	(mÅ)	(mÅ)	(K/H)	($\times 10^{12} \text{ cm}^{-2}$)
-77	241 ± 3	279 ± 3	1.16	> 2.4	42 ± 3	73 ± 3	1.74	> 2.6
-51	278 ± 3	312 ± 4	1.12	> 0.9	110 ± 3	166 ± 4	1.51	> 2.4

Computed from $^\dagger\text{Na I D1}$ and $^\ddagger\text{Ca II H}$

Table 2. Equivalent widths and column density lower limits of the Na I D and Ca II H&K features with centroids at -77 and -51 km s^{-1} . The line ratios are indicative of optically thick gas clouds, precluding us from computing exact column densities.

Models of CS gas surrounding SNe Ia suggest that photoionisation should lead to a complete disappearance of absorption features by the time the explosion reaches maximum brightness (Borkowski et al. 2009; Ferretti et al. 2016). Thus the remote location and early discovery of iPTF16abc made it an ideal SNe Ia candidate to search for CS matter by looking for changes in absorption line profiles.

To detect photoionisation, spectra are required to be obtained early, have good a signal-to-noise ratio and high resolution. At early phases (around -14 days), most SNe Ia are still too faint to be observed with high-resolution spectrographs. However the combination high-resolution spectra at maximum light with lower resolution (but high signal-to-noise) spectra at earlier times, allows for optimal coverage of the phases during which photoionisation might occur.

In Table 3, we present the time series of the measured EWs of Na I D and Ca II H&K. It can be seen that there is neither significant time variability in the EW measurements, nor are there any visible changes in the line profiles.

Because different absorbers do not have the same ionisation energies, their ionisation rates differ. It is thus possible to exclude

the presence of gas at different radii by searching for variations in the absorption by several species.

Using the method of Ferretti et al. (2016), we can exclude the presence of Na I gas at a distance of $R_{\text{Na I}}^{\text{excl}} \approx 1 \times 10^{18} - 1 \times 10^{19} \text{ cm}$, and Ca II gas at $R_{\text{Ca II}}^{\text{excl}} \approx 8 \times 10^{16} - 3 \times 10^{17} \text{ cm}$ from iPTF16abc to 3σ . The exclusion limits do not include possible errors in the SNe Ia SED as described in Ferretti et al. (2016). In particular, the exclusion limits obtained from Ca II must be taken with caution, due to the diversity of the SNe Ia SEDs.

The inner radius limit implies that all gas must have ionised before the first Xshooter spectrum was obtained. Thus all the detected absorption features must originate from gas farther from iPTF16abc than the outer exclusion limit. Due to the broad nature of intrinsic supernova spectral features, it is not possible to further determine the systemic velocity of the supernova with respect to the gas clouds. It is nevertheless plausible that the progenitor system of iPTF16abc was moving with the tidally stripped gas behind which it exploded.

Instrument	Date	Phase (days)	R ($\lambda/\delta\lambda$)	S/N	Na I D1 (mÅ)	Na I D2 (mÅ)	Ca II H (mÅ)	Ca II K (mÅ)
XShooter	Apr. 14	-6.1	7,450 [†]	113	512 ± 6	606 ± 6	141 ± 4	238 ± 8
UVES	Apr. 16	-3.6	68,000	20	517 ± 7	585 ± 7	147 ± 7	240 ± 6
UVES	Apr. 24	4.3	87,000	25	511 ± 5	597 ± 5	155 ± 6	238 ± 6
XShooter	May 12	21.2	7,450 [†]	73	497 ± 10	592 ± 10	138 ± 8	227 ± 9
Average					511 ± 3	597 ± 3	145 ± 3	237 ± 3

[†]nominal XShooter resolution

Table 3. Equivalent widths of Na I D, Ca II H&K, of iPTF 16abc using XShooter and UVES. The resolution of the UVES spectra were estimated from the full width at half-maximum intensity (FWHM) of several telluric features, and the S/N per pixel is measured around the wavelength of Na I D.

5. Discussion

The position of iPTF16abc suggests that we are probing the ISM in the tidal arm of NGC 5221. iPTF16abc is 170'' from the core of NGC 5221, which at a redshift of $z = 0.0234$ (Courtois & Tully 2015), corresponds to at least 80 kpc.

The absorption lines span a radial velocity of $-100 - -30 \text{ km s}^{-1}$, with respect to the rest-frame of the host galaxy core. These values are smaller than the rotation velocity of NGC 5221. Courtois & Tully (2015) quote a line width (twice the rotation velocity) of $510 \pm 20 \text{ km s}^{-1}$. Furthermore, two Sloan Digital Sky Survey (SDSS) spectra of spiral arms on opposite sides of the galaxy show a velocity difference of 477 km s^{-1} . The coordinates at which the SDSS spectra have been taken prior to explosion, are marked in Figure 1, whereby the eastern arm (S1) is approaching and the western arm (S2) is receding with -254 and 223 km s^{-1} , respectively.

To further compare the radial velocity of the gas seen in the iPTF16abc spectra with NGC 5221, we consider an H I profile by the Arecibo L-band Feed Array (ALFA) as part of the Arecibo Legacy Fast ALFA survey (ALFALFA, Giovanelli et al. 2005; Haynes et al. 2011). The beam of the ALFA encompasses both the position of iPTF16abc and NGC 5221. In Figure 3, the Na I D1 profile of the iPTF16abc line-of-sight is compared to the ALFA H I profile of the entire galaxy.

The position of iPTF16abc allows us to estimate a time-frame within which the gas must have been stripped from NGC 5221. Assuming the gas is moving away from the galaxy with a velocity of $v \approx 100 \text{ km s}^{-1}$, it would take at last 8×10^8 years to reach a distance of 80 kpc, depending on the exact projection angle. Models show that this time frame is consistent with close encounters and mergers of large galaxies (Toomre & Toomre 1972).

A number of galaxies, listed in Table 4, are at a comparable redshift to NGC 5221 and within a few hundred kpc from it. The two most prominent galaxies among the list, NGC 5222 and NGC 5230, are likely candidates to have interacted with NGC 5221, producing the observed tidal stream. Hallenbeck et al. (2016) have studied NGC 5230 as an example of a very H I rich galaxy. In fact, the ALFALFA data they present in their study shows that H I gas encompasses the entire galaxy group, with column density maxima corresponding to NGC 5221, NGC 5222 and NGC 5230. Thus the gas along the line-of-sight of iPTF16abc is representative of gas that can end up in the CGM of the group via interactions between the galaxies.

Narrow absorption lines, such as those detected in the spectra of iPTF16abc, are not unusual features for SNe Ia spectra (e.g. the sample of Sternberg et al. 2011). However, these features typically appear in lines-of-sight of supernovae clearly situated within their host galaxies. The Na I and Ca II gas columns

along the line-of-sight of iPTF16abc appear to be comparable to typical lines-of-sight within galaxies. To illustrate this, we consider the Na I D absorption in the two SDSS spectra available of NGC 5221. We find that the Na I D EWs of 2.1 ± 0.5 and $2.9 \pm 0.9 \text{ \AA}$ for the eastern and western spectra respectively. Ca II H&K lines are unfortunately buried in noise in the SDSS spectra and cannot be measured.

Although the Na I columns in the tidal stream and the NGC 5221 differ by close to an order of magnitude, it is important to note the differences between the SDSS and supernova Na I D EWs. In the case of the SDSS spectra, the absorption lines represent the average absorption along the lines-of-sight to all stars covered by the spectral fibre. The investigated column can thus be considered to be the average across an area of $\approx 6 \text{ kpc}^2$ area of the galaxy. In comparison to this, the column measured by the the supernova spectrum, spans the projected area of a photosphere which is of the order of $\approx 10^{-6} \text{ pc}^2$ at maximum brightness¹. We are thus comparing a very small area in the tidal tail to the average of a large area within the galaxy, where many more gas clouds with different velocities can be situated along the line-of-sight.

From ISM studies of the Milky Way, it is known that Na I D and Ca II H&K correlate with reddening and also H I column densities (Poznanski et al. 2012; Murga et al. 2015, respectively). These empirical relations can be used to estimate $E(B - V)$ and $N(\text{H I})$ for the line-of-sight of iPTF16abc. Since Na I D and Ca II H&K of iPTF16abc are optically thick, only lower limits can be computed and are presented in Table 5.

It is known that the empirical relations of Na I D to reddening work poorly for SNe Ia (Poznanski et al. 2011; Phillips et al. 2013). iPTF16abc is another example with deep Na I D absorption lines, but comparatively little photometric reddening. The H I column density estimates are more difficult to compare to. From the ALFA spectrum, we can compute that the entire beam, spanning $3.5' \times 3.8'$ contains $M_{\text{H I}} = 1.0 \times 10^{10} M_{\odot}$, corresponding to an average column density of $N(\text{H I}) = 3.7 \times 10^{19} \text{ cm}^{-2}$. Most of the H I in the ALFA spectrum must be situated in NGC 5221, but could also have been stripped to locations such as the line-of-sight of iPTF16abc. Assuming the Murga et al. (2015) relations, this must be the case with $N(\text{H I})_{\text{est.}} > 10^{21} \text{ cm}^{-2}$.

6. Summary and conclusions

We have presented the interstellar absorption lines observed in the spectra of type Ia supernova iPTF16abc. The gas corresponds to the tidally stripped ISM 80 kpc from the host galaxy NGC 5221. We detected Na I D and Ca II H&K absorption features in two distinct clusters at velocities -77 and -51 km s^{-1}

¹ Approximated from 10^4 km s^{-1} expansion after 21 days.

Galaxy	Redshift	perp. Dist. [†] (kpc)	Direction	Morphology / Notes
2MASX J13341283+1349334	0.0235	296	W	dwarf
2MASX J13343006+1348154	0.0242	184	WSW	?
SDSS J133443.53+134507.3	0.0253	161	SW	? elongated dwarf
2MASX J13344815+1344391	0.0222	159	SSW	dwarf
NGC 5222	0.0231	154	S	large elliptical
–	0.0228	150	S	irregular overlapping merging with NGC 5222
NGC 5230	0.0229	363	SE	large face-on spiral
SDSS J133509.69+135324.0	0.0234	136	NE	dwarf
NGC 5226	0.0244	161	NNE	spiral?

[†]At $z = 0.0234$.

Table 4. Neighbouring galaxies of NGC 5221 at comparable redshift.

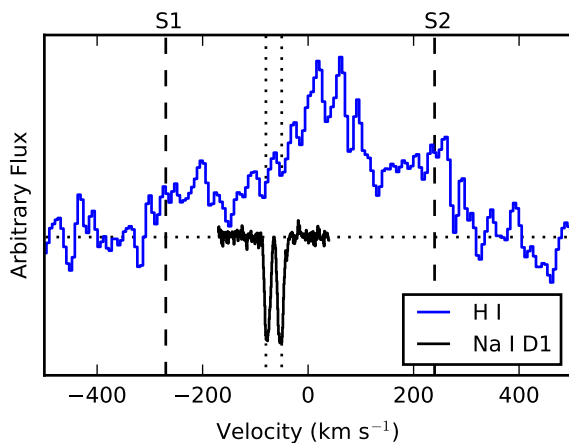


Fig. 3. Comparison of the radial velocity of the Na I gas along the line-of-sight of iPTF16abc and H I in and around NGC 5221. The ALFA H I spectrum encompasses the position of iPTF16abc and NGC 5221. The Na I D1 profile is shown from the Apr. 24 UVES spectrum. Vertical dashed lines indicate the line-of-sight velocity of the two SDSS spectra of NGC 5221, with labels S1 and S2 corresponding to those in Figure 1.

Feature	avg. EW (mÅ)	Est. $E(B - V)$ (mag)	Est. $N(\text{H I})$ ($\times 10^{21} \text{ cm}^{-2}$)
Na I D1	511 ± 3	> 0.32	> 1.2
Na I D2	597 ± 3	> 0.24	> 1.1
Ca II H	145 ± 3	–	> 0.23
Ca II K	237 ± 3	–	> 0.22

Table 5. Estimated reddening and H I column densities based on relations of Poznanski et al. (2012) and Murga et al. (2015), respectively.

from the systemic velocity of NGC 5221. We also detect K I and a DIB at $\lambda 6284$, which are also typical constituents of interstellar media, while reddening due to dust appears to be negligible. Due to the standard candle nature of SNe Ia, we can also exclude the presence of grey dust, since the extinction is negligible. If grey dust is to play a significant role in the intergalactic medium, over densities could be expected in the environment of iPTF16abc. We have shown that this unique line-of-sight, far from a host galaxy, can have the same ISM properties as a line-of-sight within a galaxy.

From the lack of variations in the Na I D and Ca II H&K profiles, we determined that the observed gas cannot be part of the CS environment of the supernova, since photoionisation would have resulted in a significant change in the column density. Thus the gas seen along the line-of-sight of iPTF16abc is the tidally stripped ISM of NGC 5221. At the same time, the lightcurves of iPTF16abc show very little reddening.

At the same time the standard candle nature of iPTF16abc has allowed us to determine that the supernova is barely reddened compared with the normal SNe Ia colours.

NGC 5221 likely had a close encounter with one of its neighbouring galaxies in the past $\approx 10^9$ years, when large portions of gas and the progenitor system of iPTF16abc were tidally stripped from it. A map of H I content of the group of galaxies including NGC 5221, presented by Hallenbeck et al. (2016), suggests that the group shares a common gas envelope. As the galaxies within the group are likely to continue to interact and merge in the future, the gas seen along the line-of-sight of iPTF16abc is representative of the gas that is transplanted into the CGM surrounding the galaxy group.

It has been shown that dense cold gas clouds can exist in the CGM of galaxy groups for $> 5 \times 10^8$ years (Borthakur et al. 2015). In future interactions with neighbouring galaxies, these clouds can be the sites of star formation. On the long run however, the gas clouds could dissipate, enriching the CGM with the detected metals.

The presented gas profiles along the line-of-sight of iPTF16abc should be useful to future studies of NGC 5221, its tidal tail and the galaxy group it is located in. In particular, the profiles could compliment higher resolution observations of the H I gas in NGC 5221 and the tidal arm, resolving the dynamics of the galaxy group.

Acknowledgements. We thank Gregory Hallenbeck for his help with extracting ALFA data and David Martinez-Delgado, Darach Watson and Brice Menard for their insights. R.A. and A.G. acknowledge support from the Swedish Research Council and the Swedish Space Board. The Oskar Klein Centre is funded by the Swedish Research Council. This work makes use of observations from the LCOGT network. The Pan-STARRS1 Surveys (PS1) and the PS1 public science archive have been made possible through contributions by the Institute for Astronomy, the University of Hawaii, the Pan-STARRS Project Office, the Max-Planck Society and its participating institutes, the Max Planck Institute for Astronomy, Heidelberg and the Max Planck Institute for Extraterrestrial Physics, Garching, The Johns Hopkins University, Durham University, the University of Edinburgh, the Queen’s University Belfast, the Harvard-Smithsonian Center for Astrophysics, the Las Cumbres Observatory Global Telescope Network Incorporated, the National Central University of Taiwan, the Space Telescope Science Institute, the National Aeronautics and Space Administration under Grant No. NNX08AR22G issued through the Planetary Science Division of the NASA Science Mission Directorate, the National Science Foundation Grant No. AST-1238877, the University of Maryland, Eotvos Lorand University (ELTE), the Los Alamos National Laboratory, and the Gordon and Betty Moore Foundation.

References

- Aguirre, A. 1999a, *ApJ*, 525, 583
 Aguirre, A. N. 1999b, *ApJ*, 512, L19
 Amanullah, R., Goobar, A., Johansson, J., et al. 2014, *ApJ*, 788, L21
 Amanullah, R., Johansson, J., Goobar, A., et al. 2015, *MNRAS*, 453, 3300
 Baron, D., Poznanski, D., Watson, D., Yao, Y., & Prochaska, J. X. 2015, *MNRAS*, 447, 545
 Borkowski, K. J., Blondin, J. M., & Reynolds, S. P. 2009, *ApJ*, 699, L64
 Borthakur, S., Yun, M. S., Verdes-Montenegro, L., et al. 2015, *ApJ*, 812, 78
 Cenko, S. B., Cao, Y., Kasliwal, M., et al. 2016, *The Astronomer's Telegram*, 8909
 Courtois, H. M. & Tully, R. B. 2015, *MNRAS*, 447, 1531
 Dekker, H., D'Odorico, S., Kaufer, A., Delabre, B., & Kotzlwski, H. 2000, in *Society of Photo-Optical Instrumentation Engineers (SPIE) Conference Series*, Vol. 4008, *Optical and IR Telescope Instrumentation and Detectors*, ed. M. Iye & A. F. Moorwood, 534
 Drake, A. J., Djorgovski, S. G., Graham, M. J., et al. 2013a, *Central Bureau Electronic Telegrams*, 3555
 Drake, A. J., Djorgovski, S. G., Mahabal, A. A., et al. 2013b, *The Astronomer's Telegram*, 5097
 Ferretti, R., Amanullah, R., Goobar, A., et al. 2016, *A&A*, 592, A40
 Flewelling, H. A., Magnier, E. A., Chambers, K. C., et al. 2016, *ArXiv e-prints*
 Foley, R. J., Fox, O. D., McCully, C., et al. 2014, *MNRAS*, 443, 2887
 Fox, O. D., Kutyrev, A. S., Rapchun, D. A., et al. 2012, in *Proc. SPIE*, Vol. 8453, *High Energy, Optical, and Infrared Detectors for Astronomy V*, 84531O
 Gehrels, N., Chincarini, G., Giommi, P., et al. 2004, *ApJ*, 611, 1005
 Giovanelli, R., Haynes, M. P., Kent, B. R., et al. 2005, *AJ*, 130, 2598
 Goldhaber, G., Groom, D. E., Kim, A., et al. 2001, *ApJ*, 558, 359
 Goobar, A., Bergström, L., & Mörtzell, E. 2002, *A&A*, 384, 1
 Goobar, A., Johansson, J., Amanullah, R., et al. 2014, *ApJ*, 784, L12
 Goobar, A. & Leibundgut, B. 2011, *Annual Review of Nuclear and Particle Science*, 61, 251
 Graham, M. L., Valenti, S., Fulton, B. J., et al. 2015, *ApJ*, 801, 136
 Guy, J., Astier, P., Baumont, S., et al. 2007, *A&A*, 466, 11
 Hallenbeck, G., Huang, S., Spekkens, K., et al. 2016, *AJ*, 152, 225
 Haynes, M. P., Giovanelli, R., Martin, A. M., et al. 2011, *AJ*, 142, 170
 Kausch, W., Noll, S., Smette, A., et al. 2015, *A&A*, 576, A78
 Kramida, A., Ralchenko, Y., J., R., & NIST ASD Team. 2014, *NIST Atomic Spectra Database (ver. 5.2)*, *NIST Atomic Spectra Database (ver. 5.2)*, [Online]. Available: <http://physics.nist.gov/asd> [2015, June 30]. National Institute of Standards and Technology, Gaithersburg, MD.
 Maguire, K., Sullivan, M., Patat, F., et al. 2013, *MNRAS*, 436, 222
 Maguire, K., Sullivan, M., Thomas, R. C., et al. 2011, *MNRAS*, 418, 747
 Maoz, D., Mannucci, F., & Brandt, T. D. 2012, *MNRAS*, 426, 3282
 Ménard, B., Kilbinger, M., & Scranton, R. 2010, *MNRAS*, 406, 1815
 Miller, A. A. ???
 Miller, A. A., Laher, R., Masci, F., et al. 2016, *The Astronomer's Telegram*, 8907
 Modigliani, A., Goldoni, P., Royer, F., et al. 2010, in *Proc. SPIE*, Vol. 7737, *Observatory Operations: Strategies, Processes, and Systems III*, 773728
 Mörtzell, E. & Goobar, A. 2003, *J. Cosmology Astropart. Phys.*, 9, 009
 Murga, M., Zhu, G., Ménard, B., & Lan, T.-W. 2015, *MNRAS*, 452, 511
 Patat, F., Chandra, P., Chevalier, R., et al. 2007, *Science*, 317, 924
 Perlmutter, S., Aldering, G., Goldhaber, G., et al. 1999, *ApJ*, 517, 565
 Phillips, M. M., Simon, J. D., Morrell, N., et al. 2013, *ApJ*, 779, 38
 Poznanski, D., Ganeshalingam, M., Silverman, J. M., & Filippenko, A. V. 2011, *MNRAS*, 415, L81
 Poznanski, D., Prochaska, J. X., & Bloom, J. S. 2012, *MNRAS*, 426, 1465
 Riess, A. G., Filippenko, A. V., Challis, P., et al. 1998, *AJ*, 116, 1009
 Ritchey, A. M. & Wallerstein, G. 2015, *PASP*, 127, 223
 Ritchey, A. M., Welty, D. E., Dahlstrom, J. A., & York, D. G. 2015, *ApJ*, 799, 197
 Roming, P. W. A., Kennedy, T. E., Mason, K. O., et al. 2005, *Space Sci. Rev.*, 120, 95
 Schlafly, E. F. & Finkbeiner, D. P. 2011, *ApJ*, 737, 103
 Schombert, J. M., Wallin, J. F., & Struck-Marcell, C. 1990, *AJ*, 99, 497
 Simon, J. D., Gal-Yam, A., Gnat, O., et al. 2009, *ApJ*, 702, 1157
 Smette, A., Sana, H., Noll, S., et al. 2015, *A&A*, 576, A77
 Snow, T. P. 2001, *Spectrochimica Acta*, 57, 615
 Snow, T. P. & McCall, B. J. 2006, *ARA&A*, 44, 367
 Sollerman, J., Cox, N., Mattila, S., et al. 2005, *A&A*, 429, 559
 Sternberg, A., Gal-Yam, A., Simon, J. D., et al. 2011, *Science*, 333, 856
 Toomre, A. & Toomre, J. 1972, *ApJ*, 178, 623
 Vernet, J., Dekker, H., D'Odorico, S., et al. 2011, *A&A*, 536, A105
 Welty, D. E., Ritchey, A. M., Dahlstrom, J. A., & York, D. G. 2014, *ApJ*, 792, 106